scientific reports

Check for updates

OPEN

Long term effects of lead contaminated water on the strength and microstructure of concrete

Sedigheh Ghasemi✉, Peyman Homami✉ & Jafar Keyvani Ghamsari

The discharge of lead-contaminated effluents from industrial activities such as smelting, refining, and petrochemical operations poses a critical environmental challenge by polluting surface and groundwater resources. Among mitigation strategies, the use of cement-based materials for the stabilization and solidification (S/S) of lead contaminants offers a promising approach, integrating environmental management with construction applications. This study systematically investigates the long-term effects of lead-contaminated mixing water on the mechanical performance, durability, and pollutant immobilization capacity of concrete, with particular focus on microstructural evolution. A total of 210 concrete specimens were prepared using mixing water containing lead concentrations of 0, 0.001, 0.002, 0.005, 0.01, 0.02, and 0.05 M. Compressive strength tests were conducted at curing ages ranging from 3 to 730 days, and pollutant retention was assessed using the toxicity characteristic leaching procedure. Microstructural analyses through X-ray diffraction, scanning electron microscopy, and energy dispersive X-ray spectroscopy revealed that lead contamination disrupted cement hydration by forming $Pb(OH)_2$ and Pb-C-S-H phases, which inhibited the nucleation and growth of primary hydration products, notably calcium silicate hydrate (C-S-H) and portlandite (CH). At 0.05 M lead concentration, a compressive strength reduction of 61% was recorded after 365 days, with further deterioration to 14 MPa after 730 days. Despite the mechanical degradation, the stabilization process significantly reduced lead leaching, maintaining compliance with environmental standards for non-structural applications. These findings highlight the feasibility of employing lead-contaminated water in controlled construction uses, while emphasizing the critical need to account for long-term mechanical performance reductions when designing S/S-based waste management solutions.

Keywords Lead-heavy metal pollutants, Cement hydration disruption, Stabilization and solidification, Concrete microstructure, Mechanical durability, XRD analysis

The rapid expansion of industrial, mining, and agricultural activities has led to a significant increase in toxic pollutants, particularly heavy metals, in the environment. Large quantities of hazardous waste are discharged into surface and underground water resources, mainly during mineral extraction, refining, and metal processing operations[1–4]. Among these pollutants, lead (Pb) poses serious risks due to its persistence, bioaccumulation potential, and detrimental effects on human health and ecosystems.

Portland cement is the backbone of modern construction, widely utilized in infrastructure and structural applications[2,5,6]. Its primary chemical constituents—tricalcium silicate (C_3S), dicalcium silicate (C_2S), tricalcium aluminate (C_3A), and tetracalcium aluminoferite (C_4AF)—undergo hydration reactions to form a solid matrix, contributing to the mechanical strength and durability of concrete[7–10]. However, the incorporation of contaminants such as heavy metal pollutants can significantly alter the hydration kinetics, setting time, and phase formation of cement-based materials, thereby impacting their long-term performance[11,12].

Heavy metals interact with cementitious phases through various mechanisms, including surface adsorption, precipitation of hydroxides, and substitution reactions within hydration products[13–15]. These interactions can lead to hydration delay, microstructural instability, and mechanical degradation of cementitious matrices. Some metals form stable hydroxides that accelerate hydration, whereas others inhibit calcium silicate hydrate (C-S-H) development, leading to reduced compressive strength and durability[16].

Faculty of Engineering, Kharazmi University, Tehran, Iran. ✉email: Std_s_ghasemi@khu.ac.ir; homami@khu.ac.ir

Type	SiO_2	Al_2O_3	Fe_2O_3	CaO	K_2O	Na_2O	SO_3	L.O.I
Cement II	22.00	5.30	4.00	65.00	0.70	0.50	2.50	2.50

Table 1. Chemical characteristics of type II portland cement.

Materials	M (g/mol)	Density (g/cm^3)	Atomic mass (Ar)	Heat of fusion (kJ/mol)	Enthalpy of vaporization (kJ/mol)	Melting point (°C)	Boiling point (°C)
$Pb(NO_3)_2$	331.21	11.34	207.2	4.77	179.5	327.46	1749

Table 2. Some characteristics of the heavy metal lead.

The stabilization and solidification (S/S) technique has emerged as a viable approach for mitigating heavy metal contamination by immobilizing pollutants within a cementitious matrix, reducing their leachability and environmental impact[2,12]. Cement, due to its high alkalinity and pozzolanic reactivity, provides a chemically stable environment for heavy metal encapsulation. The effectiveness of S/S depends on various factors, including cement composition, curing conditions, pollutant concentration, and microstructural evolution during hydration[17].

The integration of heavy metal-laden water in cement-based materials presents both challenges and opportunities. While lead pollution in mixing water can adversely affect cement hydration and reduce mechanical performance, it also provides an opportunity for developing sustainable construction practices that utilize industrial byproducts while ensuring environmental safety[18–20]. Previous research has primarily focused on the general effects of heavy metals on cementitious materials; However, long-term and integrative microstructural assessments of lead-contaminated concrete—particularly those combining hydration analysis, pollutant retention, and mechanical performance—remain limited in the existing literature[21–23].

This study aims to address existing knowledge gaps by systematically evaluating the long-term impact of lead-contaminated mixing water on cement hydration, mechanical properties, microstructural evolution, and pollutant retention mechanisms. Specifically, the objectives are: (1) to determine the changes in compressive strength of concrete samples over a 730-day curing period under different lead concentrations; (2) to analyze the formation and transformation of hydration products, including Pb-C-S-H and $Pb(OH)_2$ phases, using XRD, SEM, and EDX techniques; and (3) to assess the long-term pollutant immobilization efficiency through TCLP leaching tests. Through this multi-faceted approach, the research seeks to answer how lead contamination affects concrete durability, microstructural integrity, and environmental compliance over extended time frames. The findings contribute to advancing the understanding of heavy metal immobilization in cementitious systems and offer practical guidance for the safe application of contaminated water in non-structural construction practices.

Materials and methods

Materials

In this study, Type II Portland cement, complying with ASTM C150 standards, was procured from Hormozgan Cement Company for concrete sample preparation. The chemical composition of the cement was analyzed using X-ray fluorescence (XRF) spectroscopy, conducted with a PHILIPS PW1410 spectrometer. The detailed oxide composition results are presented in Table 1.

In this study, the mixing water was either distilled (pH = 7) or artificially contaminated with lead nitrate ($Pb(NO_3)_2$), a representative heavy metal pollutant commonly found in industrial wastewater. The lead nitrate used was of analytical reagent grade (EMSURE® ACS, Reag. Ph Eur) and was sourced from Merck KGaA, Germany (Catalog No. 1.07398.1000, Lot No. K51636598). Its purity was greater than 99.5%, ensuring high reliability for experimental use.

No additional pre-treatment was applied to the lead nitrate; it was used directly as received from the manufacturer.

The physicochemical characteristics of lead nitrate, including its molecular weight (331.21 g/mol), atomic mass (207.2), density (11.34 g/cm^3), melting point (327.46 °C), and boiling point (1749 °C), are listed in Table 2. This selection ensures relevance to real-world heavy metal contamination scenarios and provides consistency with typical conditions found in industrial effluents.

The aggregates used in this research included natural sand (4.75–0.075 mm) and crushed gravel (9.5–4.75 mm), in accordance with ASTM C33 grading requirements[24]. The particle size distribution of the fine and coarse aggregates is illustrated in Fig. 1.

Preparation of tests

In this study, seven distinct concrete mix designs were formulated to evaluate the influence of lead-heavy metal contamination on the engineering and microstructural properties of concrete. Lead-contaminated mixing water was prepared using aqueous solutions of $Pb(NO_3)_2$ at molar concentrations of 0, 0.001, 0.002, 0.005, 0.01, 0.02, and 0.05, representing typical industrial contamination levels. The mix proportions were established in accordance with the Iranian Concrete Code (ABA) and ASTM standards, as summarized in Table 3.

In a controlled laboratory setting, raw materials were precisely weighed according to the designated mix proportions. The mixing process was conducted using a high-performance rotary mixer to ensure homogeneity

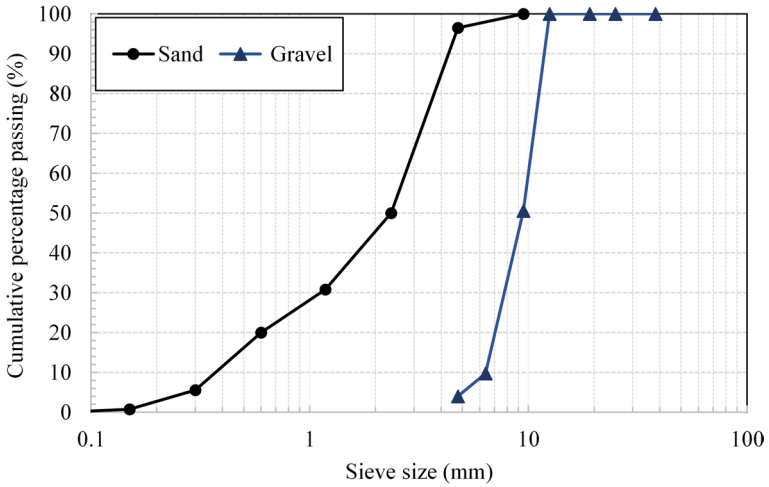

Fig. 1. Granulation curve of stone materials (sand and gravel).

Constituents	Cement (kg/m³)	Water (kg/m³)	Gravel (kg/m³)	Sand (kg/m³)	W/C	Fineness modulus
Concrete	300	144	960	800	0.48	3.2

Table 3. Concrete mixing plan with Portland cement type II.

of the cementitious matrix. The fresh concrete was cast into standard molds of dimensions 15 cm × 15 cm × 15 cm, followed by mechanical compaction to minimize entrapped air voids.

A total of 170 concrete specimens were prepared with lead-contaminated water, while 40 control specimens were produced using distilled water. After 24 h of initial setting, the specimens were demolded and subjected to water curing at 23 ± 2 °C for 3, 7, 14, 28, 90, 365 and 730 days. This comprehensive curing protocol allowed for both short-term and long-term performance assessments of the concrete mixtures.

The water-to-cement (W/C) ratio was maintained at 0.48 to ensure consistency across all test specimens. The concrete was designed with Type II Portland cement and a fineness modulus of 2.3, adhering to ASTM C204-07 specifications[24]. The produced concrete was non-air-entrained, ensuring a controlled evaluation of hydration and strength development.

Upon completion of curing, the concrete samples underwent a series of mechanical and microstructural evaluations, including[24–27]:

- Compressive strength testing (ASTM C39) using a fully automated hydraulic press.
- X-ray diffraction (XRD) analysis for phase identification of hydration products.
- Scanning electron microscopy (SEM) imaging to assess the morphological alterations induced by lead contamination.
- Energy dispersive X-ray spectroscopy (EDX) to analyze elemental distribution and heavy metal retention.
- Toxicity characteristic leaching procedure (TCLP) tests to determine lead leachability and environmental compliance.

For microstructural analysis, SEM, XRD, and EDX tests were conducted on specimens cured for 90 days to capture the long-term effects of lead contamination on cement hydration and phase evolution.

It is worth mentioning that performing TGA and FTIR tests could have provided more detailed and accurate insights into the thermochemical analysis and evolution of hydration phases, which could have contributed to enhancing the interpretation of the results. However, due to the limitations in this study, these tests were not performed.

Methodology

To perform the compressive strength test, the samples were prepared in accordance with ASTM C39 standards under laboratory conditions, following the mixing scheme outlined in Table 3[24]. The test was carried out using an automatic digital concrete breaker jack manufactured by Azmon Company. The loading speed was set at 300 kg/s for cubic samples measuring 15 cm × 15 cm × 15 cm.

After the compressive strength test, fractured concrete samples were collected for microstructural analysis. To focus on the cementitious matrix and minimize the influence of coarse aggregates, fragments rich in cement paste were carefully selected. These fragments were gently ground using a mechanical grinder to obtain a fine powder with particle sizes smaller than 0.4 mm. The samples were then oven-dried at 50 °C for 48 h, followed by vacuum exposure at approximately 0.1 bar pressure for 8 h. The resulting powder samples were subsequently used

for X-ray diffraction (XRD), scanning electron microscopy (SEM), and energy dispersive X-ray spectroscopy (EDX) analyses.

For XRD sample preparation, approximately 5 g of each sample was weighed with an accuracy of 0.001 g and exposed to radiation with a wavelength of 1.54 Å (Cu-Kα) in the 2θ range of 5° to 60°. The samples were tested using an X-ray diffractometer model D8-ADVANCE from Bruker, Germany[26].

For SEM imaging, 1 g of each sample was weighed with an accuracy of 0.001 g, coated with a thin gold layer to improve conductivity, and examined using a TESCAN Vega3 scanning electron microscope[27].

To analyze the structural and chemical characteristics of concrete samples, the EDX test was performed on 90-day cured samples to assess the elemental composition of cement hydration products and lead distribution. All microstructural tests (SEM, XRD, and EDX) were conducted at the central laboratory of Shiraz University.

The pollution leaching test was conducted based on the EPA-1311 standard to determine hazardous waste characteristics. The leaching solution was prepared by diluting 11.4 mL of acetic acid (CH_3CH_2OOH) in 2 L of distilled water, achieving a pH of 2.18 ± 0.5. The ground concrete sample was mixed with the leaching solution at a 20:1 liquid-to-solid ratio in 1-L high-density polyethylene (HDPE) containers and stirred thoroughly using a horizontal vibrating device for 18 h.

The samples were then centrifuged at 3000 rpm to separate the liquid phase from the solid phase. The lead ion concentration in the liquid phase was measured using an atomic absorption spectrometer (AAS) model GBC 932 AB Plus. To determine the amount of deposited lead, the pH of the extracted liquid was adjusted to ~ 2 using nitric acid, and the amount of lead leached was analyzed by atomic absorption spectroscopy[2].

Discussion and examination of the results

Examining the X-ray diffraction (XRD) curve of concrete samples under the influence of lead heavy metal pollutant

The X-ray diffraction (XRD) analysis results for 90-day cured concrete samples containing varying concentrations (0–0.05 M) of lead nitrate ($Pb(NO_3)_2$) are presented in Fig. 2. Portland cement primarily consists of alite (C_3S), belite (C_2S), aluminate (C_3A), and ferrite (C_4AF), which undergo hydration reactions to form the cement matrix. The reaction of C_3S and C_2S with water produces hydrated calcium silicate (C-S-H) and portlandite ($Ca(OH)_2$ or CH), which are essential for strength development. Hydration of C_3A results in the formation of hydrated calcium aluminate (C-A-H)[8].

The ferrite (C_4AF) content in cement is relatively low and does not significantly influence overall cement hydration. However, in the presence of gypsum and sulfate, aluminate and ferrite phases react to form ettringite,

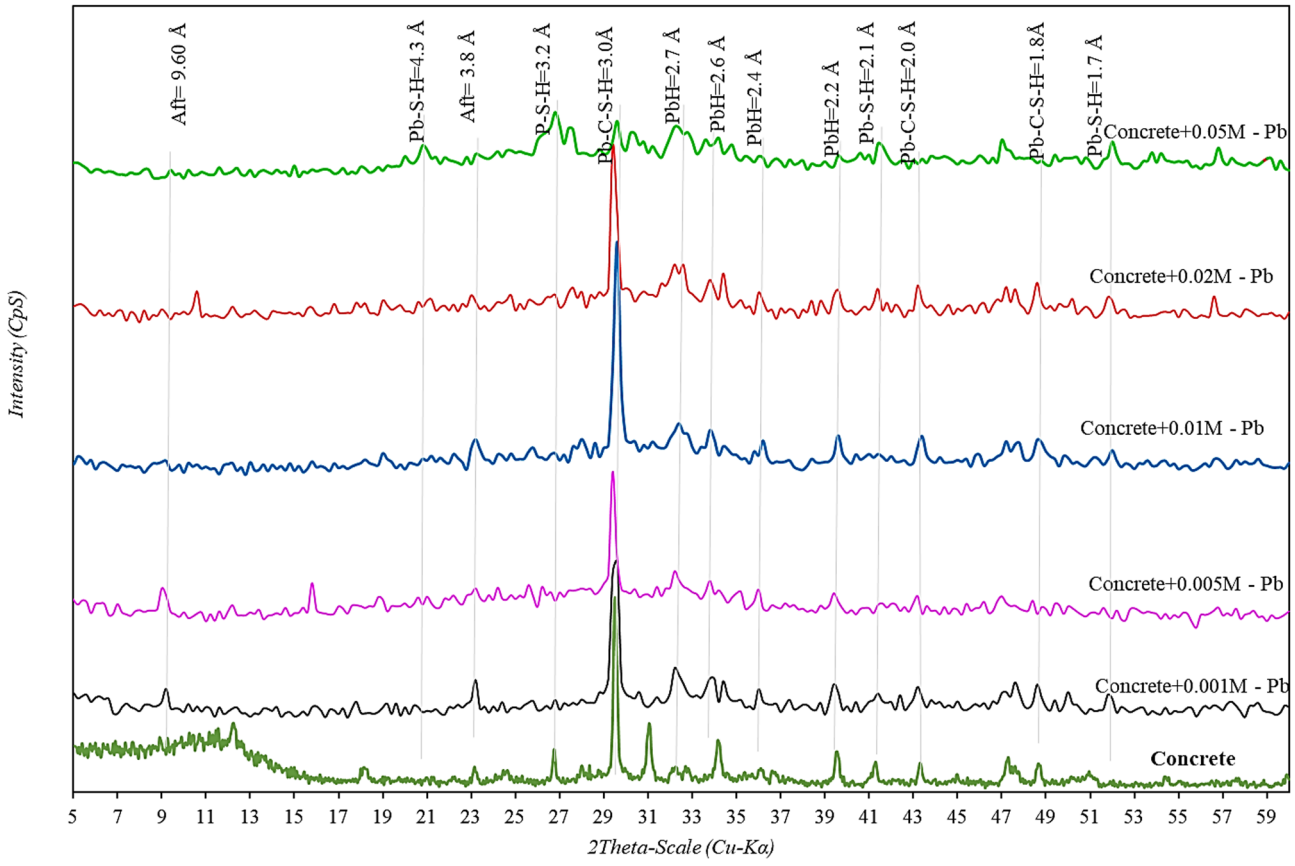

Fig. 2. X-ray diffraction (XRD) pattern of cement-lead nitrate mixture. Aft: Ettringite, Pb-S-H: lead silicate hydrate, Pb-C-S-H: lead + calcium silicate hydrate, PbH: lead hydroxide.

which contributes to early strength gain. The presence of lead-heavy metal pollutants in the mixing water disrupts these hydration reactions, affecting C-S-H and CH formation and potentially altering the cement matrix structure.

In the XRD pattern of the control sample (free of lead contamination), a prominent peak for C-S-H appears at 3.02 Å with an intensity of 521 CpS. Peaks corresponding to portlandite (CH) are observed at 4.2 Å and 3.2 Å, confirming the expected hydration process in an uncontaminated cement matrix.

In contrast, the XRD curves of lead-contaminated samples reveal the formation of Pb-C-S-H phases at 0.3 Å, 2.4 Å, 2 Å, 1.8 Å, and 1.7 Å. Peaks corresponding to lead hydroxide ($Pb(OH)_2$) appear at 4.8 Å, 2.6 Å, 2.5 Å, and 1.8 Å, indicating modifications in the hydration mechanism. Additionally, ettringite formation is observed at 3.8 Å, suggesting further microstructural alterations[1,28].

For the sample containing 0.001 M lead nitrate, a Pb-C-S-H peak is detected at 0.3 Å with an intensity of 850 CpS[21–23]. As lead concentration increases, this peak intensity rises to 850 CpS and 940 CpS in samples with 0.01 M and 0.05 M lead nitrate, respectively. The C-S-H nanostructure plays a crucial role in the stabilization and solidification of lead contaminants, and its formation is governed by Eq. (1)[1,21,28,29]:

$$\begin{aligned} &\text{C-S-H} + \text{Pb}^{2+} \rightarrow \text{Pb-C-S-H} \\ &\text{C-S-H} + \text{Pb}^{2+} \rightarrow \text{Pb-C-S-H} + \text{Ca}^{2+} \end{aligned} \tag{1}$$

The incorporation of lead into the C-S-H structure occurs via calcium substitution, inducing silicate polymerization and slowing hydration kinetics. The extent of Pb-C-S-H formation depends on pollutant concentration and solution pH. Beyond a certain lead concentration, peak intensity decreases due to Pb bond instability and partial Pb-C-S-H dissolution, affecting cement setting time[21,29].

These interpretations align with the findings of Lee[21] and Wang et al.[30], who reported that in cementitious systems exposed to lead contamination, C-S-H and Pb-C-S-H phases are generally amorphous or poorly crystalline, and thus appear as broad humps rather than distinct diffraction peaks in XRD spectra. Moreover, weak reflections corresponding to phases such as $Pb_8Ca(Si_2O_7)_3$ may occasionally emerge at higher lead concentrations, but their intensity remains low due to structural disorder. The interpretation of such patterns requires a multi-technique approach, combining XRD with SEM, EDS, and mechanical testing for robust phase confirmation.

In lead-contaminated samples, portlandite (CH) peaks are absent, whereas $Pb(OH)_2$ peaks become more prominent. The intensity of $Pb(OH)_2$ at 4.8 Å increases from 230 CpS (0.001 M) to 235 CpS (0.01 M) and 496 CpS (0.05 M), respectively. The formation of $Pb(OH)_2$ results from interactions between lead ions (Pb^{2+}), hydroxyl ions (OH^-), and calcium ions (Ca^{2+}), leading to the precipitation of $Pb(OH)_2$ and $CaPb_2(OH)_x{\cdot}yH_2O$, as shown in Eq. (2)[1,28]:

$$\begin{aligned} &\text{OH}^- + \text{Pb}^{2+} \rightarrow \text{Pb}\,(\text{OH})_2 \\ &\text{OH}^- + \text{Ca}^{2+} + \text{Pb}^{2+} \rightarrow \text{CaPb}_2\,(\text{OH})_x \cdot \text{yH}_2\text{O} \end{aligned} \tag{2}$$

Although nitrate ions (NO_3^-) were introduced through $Pb(NO_3)_2$ and are often considered as spectator ions due to their high solubility in alkaline cementitious environments, studies have shown that they may participate in ion exchange reactions with AFm phases and could influence early hydration processes. Therefore, their behavior should not be dismissed without appropriate mechanistic justification[21,29,31].

Cement plays a key role in stabilizing and solidifying lead pollutants by forming low-solubility lead hydroxide, which influences the cement hydration process and compressive strength. As lead nitrate concentration increases, the intensity of lead hydroxide peaks decreases due to pH variations, resulting in partial dissolution of lead hydroxide.

Previous studies on the effect of lead nitrate on the hydration products of aluminate and ferrite phases, particularly ettringite, have reported varying results. However, with increasing lead contamination, ettringite formation is progressively inhibited. The ettringite peak at 3.8 Å in the control sample exhibits an intensity of 68 CpS, but its intensity decreases with higher lead concentrations, indicating a disruption in its stability (Fig. 2). Therefore, the stabilization and solidification of lead occur primarily through the formation of Pb-C-S-H and lead hydroxide, with a noticeable reduction in ettringite formation affecting aluminate and ferrite hydration reactions.

Investigating the morphology of concrete samples containing different concentrations of lead heavy metal pollutant

Scanning electron microscope (SEM) images of concrete samples prepared with lead-contaminated water at varying concentrations (0–0.05 M) and a control sample at 90 days are presented in Fig. 3. As observed, the morphology of the samples changes as a function of lead concentration. Figure 3a depicts the morphology of the control sample prepared with distilled water, where the primary hydration products, including the spongy nanostructure of calcium silicate hydrate (C-S-H) and distinct calcium hydroxide (CH) crystals, are clearly visible[32]. Based on the conducted studies, four types of C-S-H are categorized according to morphology[18]: (1) Fibrous; (2) Honeycomb network; (3) Uniform particle morphology; and (4) Inner product morphology. The surface area of the C-S-H nanostructure at points 1 and 2 is approximately 15 and 40 μm^2, respectively.

The surface areas of C-S-H nanostructures at points 1 and 2 are approximately 15 μm^2 and 40 μm^2, respectively. After 90 days of hydration, the C-S-H nanostructure in the control sample shows growth due to the completion of hydration, reducing porosity and enhancing mechanical stability. The absence of cracks and defects in the

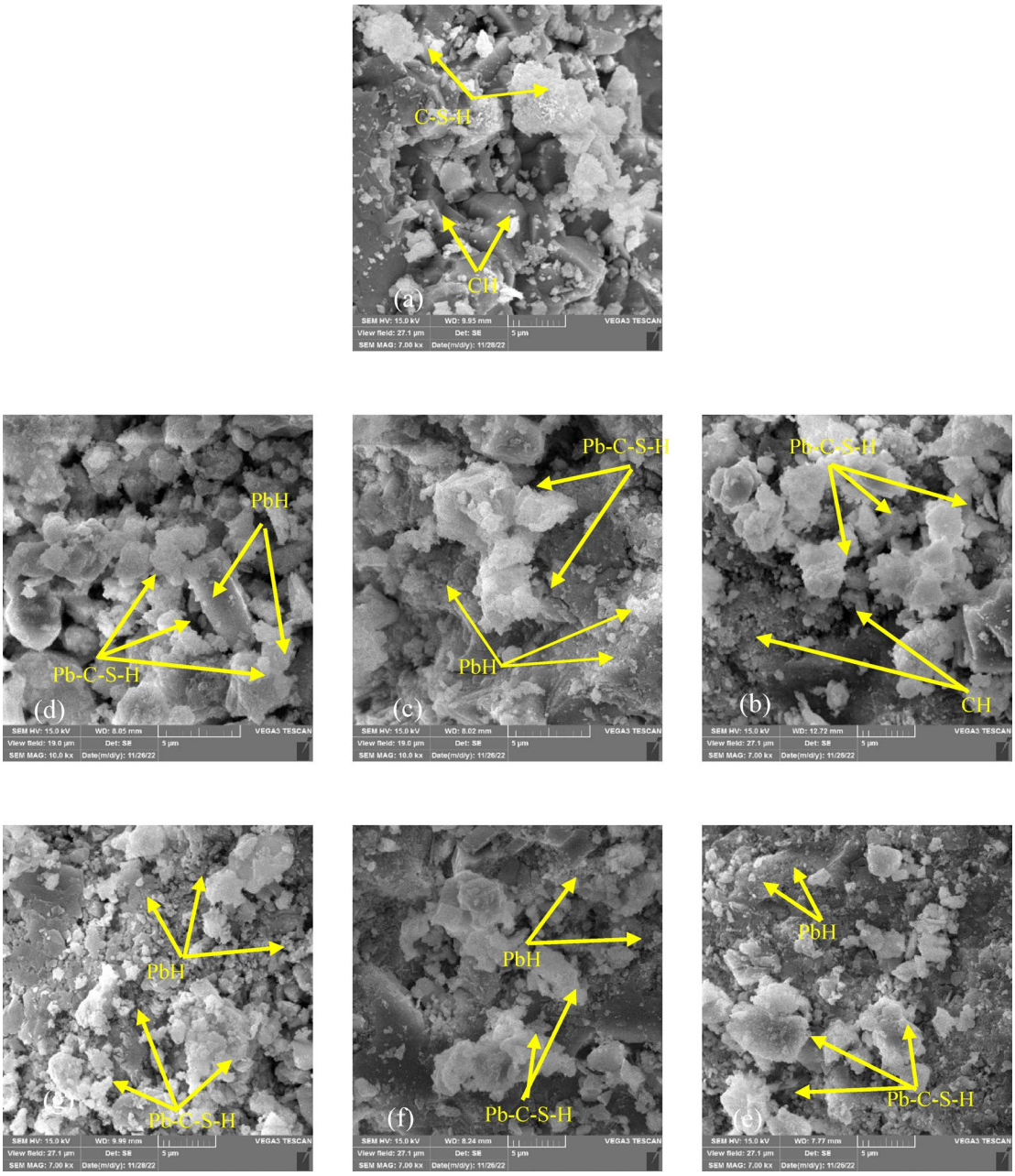

Fig. 3. SEM images of 90-day samples prepared with different concentrations of lead heavy metal pollutant pollutant (**a**) control sample, (**b**) containing 0.01 M, (**c**) 0.02 M, (**d**) 0.05 M, (**e**) 0.01 M, (**f**) 0.02 M, (**g**) 0.05 M lead nitrate.

microstructure is attributed to the dense C-S-H network, which enhances the material's absorption capacity and specific surface area.

Figure 3b–g illustrate the morphology of concrete samples prepared with different lead concentrations. Figure 3b corresponds to the sample with 0.001 M lead nitrate, where large, clotted, and irregular Pb-C-S-H nanostructures are visible. The presence of lead ions in the C-S-H phase occurs due to their atomic radius similarity to calcium, facilitating Pb incorporation and encapsulation within the cementitious matrix[21,31]. Additionally, lead hydroxide (PbH) appears as integrated microcrystals within the cement paste[33]. The precipitation of lead nitrate as $Pb(OH)_2$, facilitated by Ca^{2+} and OH^- ions released from C_3S and C_2S hydrolysis, highlights cement's capability in stabilizing lead pollutants[21,34].

X-ray energy dispersive spectroscopy (EDX) was conducted to analyze the chemical composition of the cementitious matrix. Figure 4 presents EDX results for 90-day cured samples, confirming the presence of C-S-H nanostructures and PbH phases. The weight ratios of Ca/Si, Ca/(Al + Si), Ca/(Al + Pb), and Ca/Pb were used to validate Pb incorporation into the cement structure.

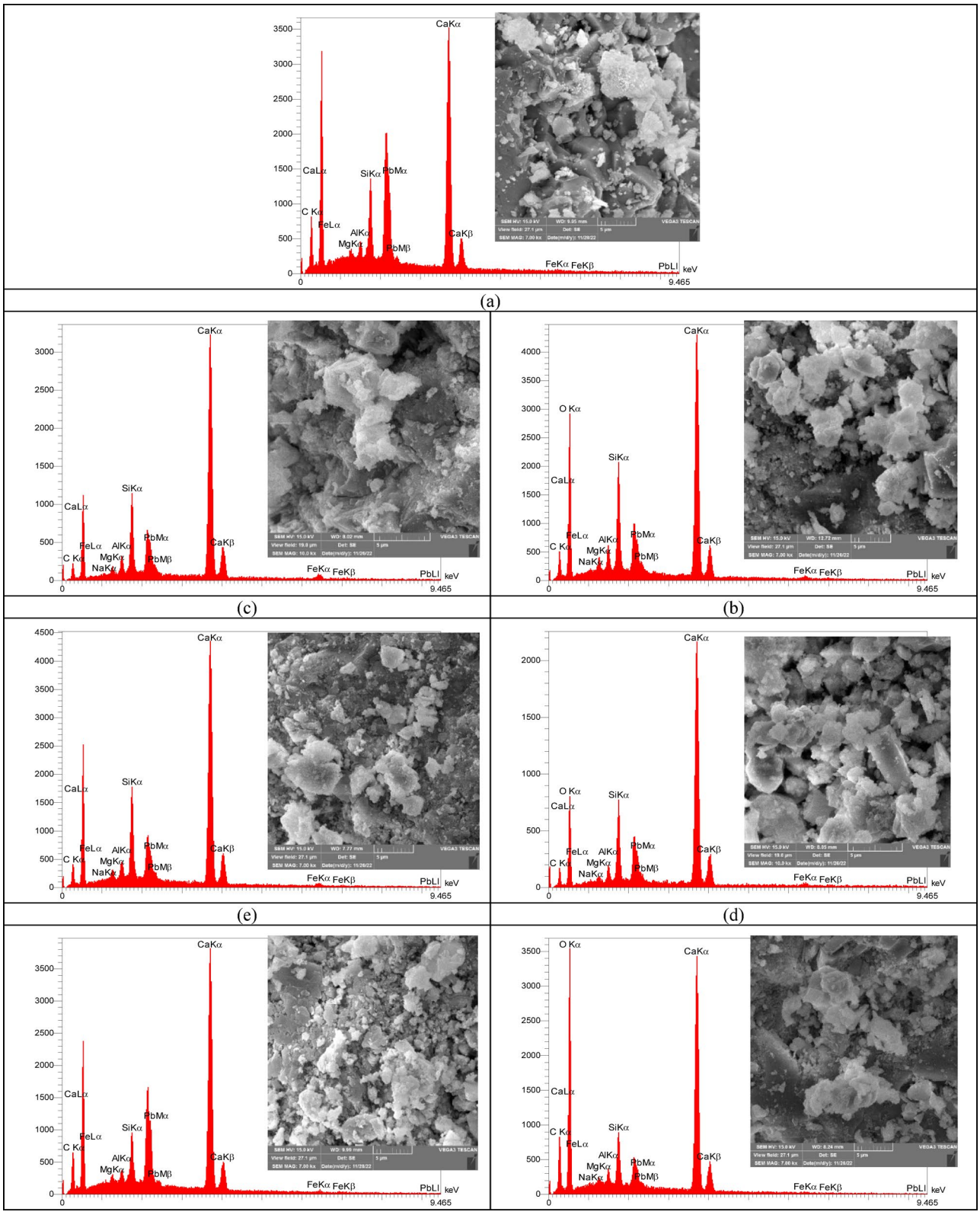

Fig. 4. EDX analysis of 90-day samples prepared with different concentrations of lead heavy metal pollutant pollutant (**a**) control sample, (**b**) containing 0.01 M, (**c**) 0.02 M, (**d**) 0.05 M, (**e**) 0.01 M, (**f**) 0.02 M, (**g**) 0.05 M lead nitrate.

The interaction between Pb^{2+}, Ca^{2+}, and OH^- leads to the formation of PbH, disrupting normal cement hydration. Another lead-bearing compound, hydrated lead silicate (Pb-S-H), forms due to alite and belite hydrolysis, appearing as polygonal sheets coated with lead[30,35]. Needle-shaped ettringite structures are visible in Fig. 3b, formed through sulfate and calcium aluminate reactions, causing volume expansion in the cement-lead mixture[30,35]. Identification of Pb-S-H and PbH phases was further confirmed by EDX weight ratios of Ca/Si, Ca/(Al + Si), and Ca/Pb (Fig. 4).

Figure 3c–g show samples with 0.002, 0.005, 0.01, 0.02, and 0.05 M lead nitrate concentrations. Pb-containing deposits cover the cement matrix, with PbH particles and coarse Pb-C-S-H grains becoming increasingly prominent at higher lead concentrations. At elevated contamination levels, lead nitrate becomes the dominant phase within the cement paste[36]. XRD and EDX results confirm that ettringite structures are absent in lead-contaminated samples due to lead salt deposition on cement hydration products, inhibiting their formation.

XRD, EDX, and SEM findings consistently demonstrate that lead pollutants up to 0.05 M are effectively stabilized within the cement matrix, forming a composite of cement hydration products and lead nitrate deposits. The stabilization process is further supported by variations in EDX weight ratios of Ca/Si, Ca/(Al + Si), and Ca/Pb. Lead primarily precipitates as $Pb(OH)_2$ and hydrated calcium silicate phases, reducing mobility and leaching potential.

In summary, lead contamination alters cement hydration kinetics, slowing the process. Higher Pb concentrations promote the formation of Pb-C-S-H nanostructures and $Pb(OH)_2$ deposits, with increased contamination levels resulting in greater lead hydrate accumulation.

Investigating the compressive strength of concrete samples containing different concentrations of lead heavy metal pollutant

The compressive strength variations of concrete samples prepared with lead-contaminated water at different concentrations (0–0.05 M), along with a control sample, were measured at 3, 7, 14, 28, 90, 365, and 730 days, as illustrated in Fig. 5. Generally, as hydration progresses, the compressive strength of all samples increases over time. In the control sample, after 3 days of curing, the compressive strength reached 24.22 MPa, increasing to 28.34 MPa, 37.85 MPa, 42.66 MPa, 44.33 MPa, and 45.8 MPa after 7, 28, 90, 365, and 730 days, respectively. The incremental strength gains for the control samples over these periods were approximately 17%, 11%, 13%, 4%, and 2%, respectively. The progressive formation of calcium silicate hydrate (C-S-H), a nanostructured hydration product sometimes referred to as a "gel," contributes to the continuous strength gain. The C-S-H-like morphology can be clearly observed in the SEM images shown in Fig. 3.

Samples containing 0.005 M lead achieved compressive strengths of 25.01 MPa, 29.62 MPa, 33.24 MPa, 34.32 MPa, and 35.10 MPa at 7, 28, 90, 365, and 730 days, respectively. Comparing the 7-day compressive strength of the control sample (28.34 MPa), the incorporation of 0.001 M lead led to a 7% reduction, decreasing the strength to 26.2 MPa. Similarly, the sample containing 0.002 M lead exhibited a compressive strength of 25.0 MPa, representing an 11% decrease compared to the control sample. At 28 days, the reduction in compressive strength became more pronounced, with the 0.001 M and 0.002 M lead-contaminated samples reaching 35.64 MPa and 32.98 MPa, respectively, indicating reductions of 6% and 12% compared to the control. These differences persisted over time, with the 0.002 M lead sample achieving only 39.12 MPa at 365 days and

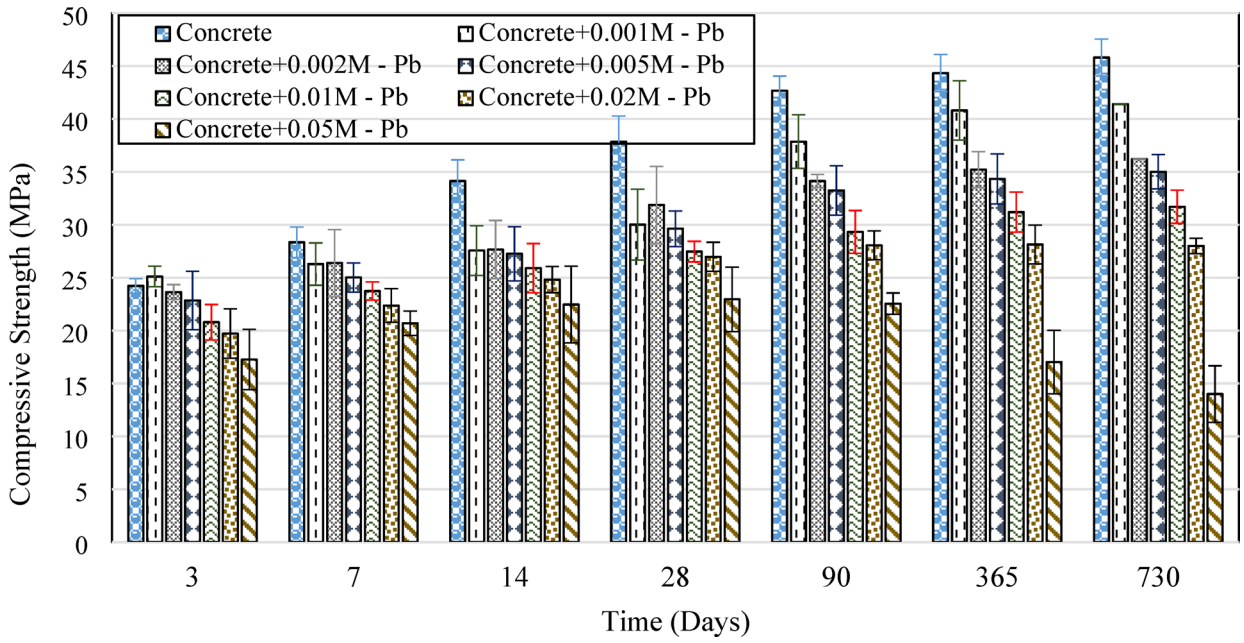

Fig. 5. Grouped bar chart showing changes in compressive strength of concrete samples containing different concentrations of lead heavy metal pollutant.

40.05 MPa at 730 days, in contrast to 44.33 MPa and 45.21 MPa for the control sample at the same ages[1,28]. The standard deviation of compressive strength values for each group ranged from 0.6 to 3.5 MPa, confirming the reliability of the measurements.

The decrease in compressive strength is primarily attributed to the high specific surface area of lead ions, which disrupts the uniform distribution of cementitious materials around aggregates. Additionally, lead contamination delays the cement hydration process, reducing the rate of C-S-H gel formation, which is crucial for strength development. This mechanism is further supported by literature indicating that Pb^{2+} incorporation into hydration products, especially C-S-H, disrupts their formation and stability[21,22]. This phenomenon is consistent with microstructural analyses, where SEM images revealed a looser and more porous microstructure in lead-contaminated samples compared to the control. Although calorimetric measurements were beyond the scope of this study, several prior works have experimentally confirmed that Pb^{2+} ions interfere with hydration kinetics and delay the formation of C-S-H and CH phases, which directly compromises strength development[21–23].

With increasing lead concentration in mixing water, compressive strength consistently declined. For instance, samples containing 0.005 M, 0.01 M, 0.02 M, and 0.05 M lead exhibited compressive strengths of 25 MPa, 23.7 MPa, 22.3 MPa, and 20.6 MPa, respectively. This trend persisted across all testing ages, highlighting the detrimental effect of lead contamination on cement hydration and mechanical performance. The decline in compressive strength is attributed to the interference of Pb^{2+} ions with the normal hydration process, particularly their interaction with calcium and hydroxide ions.

At 90 days of curing, the compressive strengths of the control sample and samples containing 0.001 M, 0.002 M, 0.005 M, 0.01 M, 0.02 M, and 0.05 M lead were recorded as 42.8 MPa, 38.37 MPa, 31.34 MPa, 32.33 MPa, 29.5 MPa, 28.5 MPa, and 23.5 MPa, respectively. The sample with 0.05 M lead exhibited the lowest compressive strength, confirming that higher lead concentrations significantly impair the mechanical integrity of concrete.

XRD and SEM analyses reveal that Pb^{2+} ions partially replace Ca^{2+} in the C-S-H nanostructure, leading to the formation of Pb-C-S-H, PbH, and Pb-S-H phases. The reaction between lead, calcium, and hydroxide ions hinders the formation of essential hydration products, resulting in the precipitation of $Pb(OH)_2$ deposits[21]. These deposits coat cementitious phases, inhibiting the development of C-S-H and CH structures, thereby delaying the setting time and reducing compressive strength[37].

Additionally, the encapsulation of lead within Pb-C-S-H and PbH deposits leads to a progressive decline in compressive strength over time[2,36,38]. SEM images confirm that PbH structures appear as fine crystalline aggregates within the cement-lead nitrate matrix[34]. The interaction of Pb^{2+} with Ca^{2+} and OH^- ions promotes the formation of PbH, preventing the normal hydration of cement. Furthermore, the hydrolysis of alite and belite results in another stable lead-bearing phase, hydrated lead silicate (Pb-S-H), which appears as polygonal sheet-like structures enveloped by lead deposits[21,29].

A detailed examination of the long-term compressive strength results in Fig. 5 indicates that at higher concentrations of the heavy metal pollutant lead, the rate of compressive strength growth becomes negative. Specifically, at a concentration of 0.05 M, the compressive strength of the samples decreased to 17.03 and 14 MPa at 365 and 730 days, respectively. This reduction corresponds to a 24% and 38% decrease in compressive strength compared to the 90-day samples at the same concentration. A similar trend is observed at a concentration of 0.02 M, although the decrease in strength is less pronounced.

Lead pollutants (Pb^{2+}) weaken the long-term strength of concrete by affecting the structure, stability, and type of C-S-H. The EDX analysis results (Fig. 4) show that the presence of lead reduces the concentration of active calcium in the cementitious structure, causing amorphization (reduction in structural order) of C-S-H, which in turn decreases its stability. Changes in the Ca/Si ratio and the morphology of C-S-H contribute to the decline in compressive strength, with C-S-H having a higher Ca/Si ratio and uniform particle structure showing higher strength compared to C-S-H with fibrous or networked structures. This trend is also confirmed in the compressive strength results, where samples containing lead exhibit a noticeably lower compressive strength compared to the control samples.

Moreover, the XRD and SEM results indicate that the presence of lead prevents the formation of ettringite and even leads to its elimination. The reduction and removal of ettringite result in increased porosity and decreased structural density of the cement paste, which directly impacts the reduction in compressive strength.

Overall, since the products of the stabilization and solidification process are sometimes used for non-construction purposes, the changes in compressive strength and its reduction should be considered a critical factor in the long-term performance evaluation of these materials.

Toxicity characteristic leaching procedure (TCLP) in the stabilization and solidification process

The rate of pollutant leaching is a critical parameter for evaluating the efficiency of the stabilization and solidification (S/S) process. Accordingly, concrete samples containing different concentrations of lead were analyzed after 28 days using the EPA-1311 standard for heavy metal leaching. Table 4 presents the results of lead leaching in cement-stabilized samples over 28 days, covering contamination levels from 0 to 0.02 M.

According to Table 4, after 28 days of processing, the leaching concentration of lead at 0.001 M was approximately 0.5 ppm. Increasing the lead content to 0.005 M resulted in a leaching rate of 5.6 ppm. At 0.01 M, the leached lead concentration reached 14.3 ppm, while at 0.02 M, it increased to 30.01 ppm. The formation of Pb-C-S-H through its reaction with C-S-H, along with $Pb(OH)_2$ precipitation, played a key role in physically encapsulating lead, contributing to its stabilization and solidification. Although NO_3^- ions are often considered as highly soluble and non-complexing in alkaline cementitious environments, recent studies have shown that they may engage in ion exchange interactions with AFm phases, particularly during early hydration stages. Therefore, their presence in the system could influence hydration kinetics and, to some extent, the distribution or retention of lead. Nevertheless, in our experiments, the overall lead leaching behavior observed in the

The concentration of lead pollutant in the sample (M)		0.001	0.002	0.005	0.01	0.02
The concentration of lead pollutant in the sample (ppm)		1036	2072	5180	10,360	20,720
pH						
2.18	Sample 1	0.53	1.32	5.58	14.22	30.41
2.15	Sample 2	0.47	1.66	5.57	14.35	29.89
2.15	Sample 3	0.50	2.14	5.82	14.25	29.74
2.16	Average	0.50	1.71	5.65	14.27	30.01
0.02	Standard deviation	0.07	0.82	0.28	0.13	0.70
–	Standard in water (ppm)	5.00	5.00	5.00	5.00	5.00
–	Standard in soil in residential environment (ppm)	50	50	50	50	50
	Standard in soil in industrial environment (ppm)	200	200	200	200	200

Table 4. Results of toxicity characteristic leaching procedure (TCLP) in samples containing different concentrations of lead heavy metal pollutant pollutant with cement after 28 days of processing.

TCLP results was not significantly altered by the presence of nitrate ions. These results were evaluated against environmental regulatory benchmarks for water and soil applications, as presented in Table 4, to assess the treatment effectiveness.

As per EPA regulations, the permissible lead concentration is 5 ppm for water and 1 ppm for drinking water. For soil contamination, the limit is 50 ppm in residential areas and 200 ppm in industrial areas. Based on these standards, leaching levels up to 0.02 M remained below the permissible thresholds for residential and industrial soil applications. However, for drinking water, only the 0.001 M concentration met the safety standard, while non-drinking water applications could tolerate up to 0.005 M through the stabilization and solidification process.

The hydration and solidification mechanisms in the cement matrix, along with pollutant retention facilitated by the C-S-H nanostructure, effectively reduced lead leaching. These findings are supported by X-ray diffraction (XRD) analysis, which confirms the immobilization of lead within the cementitious matrix during the S/S process.

The compressive strength of concrete samples was significantly affected by the presence of lead contaminants in the mixing water. Table 5 presents the compressive strength values, percentage reduction compared to the control sample, microstructural analysis results, and TCLP test data.

As observed, the control sample (0 M lead) exhibited normal cement hydration products, including calcium silicate hydrate (C-S-H) and portlandite (CH). Its compressive strength consistently increased over time, reaching 44.33 MPa at 365 days and 45.8 MPa at 730 days.

In contrast, lead-contaminated samples showed a significant reduction in compressive strength, which correlated with lead concentration. For example, the sample with 0.001 M lead showed a 7.3% reduction at 7 days, which improved to a 9.6% reduction at 730 days. At higher contamination levels, such as 0.05 M lead, compressive strength decreased by 61.6% at 365 days and reached a 69.4% reduction at 730 days, indicating severe long-term durability issues.

At high Pb concentrations (≥ 0.01 M), long-term compressive strength showed a drastic reduction ($> 30\%$) compared to the control. XRD and SEM analyses confirmed the formation of Pb-containing phases, such as Pb-C-S-H and $Pb(OH)_2$, which disrupted normal hydration by reducing CH and encapsulating cementitious phases. Increasing Pb concentration led to greater amorphization of the C-S-H phase, a reduction in the Ca/Si ratio, and accelerated structural deterioration over time. The presence of these compounds was associated with the observed strength reduction, highlighting the adverse impact of lead contamination on the cementitious matrix.

Additionally, TCLP test results showed that while the stabilization and solidification process effectively immobilized lead within the concrete matrix, the leaching rate increased with higher lead concentrations. Even at 0.05 M lead, the leaching rate reached 14.3 ppm at 28 days but remained below regulatory limits, indicating that such contaminated water could still be used in non-structural applications under appropriate environmental standards.

The highest Pb concentration (0.05 M) resulted in almost 70% strength loss after 2 years, indicating severe durability issues. These findings emphasize the necessity of evaluating heavy metal contaminants in concrete and demonstrate that while lead contamination significantly degrades mechanical performance, proper management strategies can mitigate environmental risks.

Conclusion

This study examined the effect of lead-contaminated mixing water on the compressive strength and microstructural characteristics of concrete, leading to the following key findings:

- The presence of lead nitrate in mixing water significantly disrupted the formation and stability of C-S-H nanostructures, leading to the development of Pb-C-S-H due to lead encapsulation within the C-S-H phase.
- XRD and SEM analyses confirmed that a portion of the lead contaminants was stabilized through precipitation mechanisms, forming lead hydroxide ($Pb(OH)_2$). These solid deposits altered the cement hydration process, reducing CH formation and modifying long-term cementitious properties, leading to progressive strength loss.

		Compressive strength (MPa)		Compressive strength changes compared to the control sample	Microstructural analysis (XRD and SEM)	TCLP leaching test (28 days)
Case 1	Control sample (0 M lead heavy metal)	3 days	24.22	–	Presence of hydrated calcium silicate (C-S-H) and portlandite (CH) Typical cement hydration observed	Lead leaching rate: Below detectable limits (compliant with standards)
		7 days	28.34	–		
		14 days	34.13	–		
		28 days	37.85	–		
		90 days	42.66	–		
		365 days	44.33			
		730 days	45.8			
Case 2	0.001 M lead heavy metal	3 days	25.1	3.63	Formation of Pb-C-S-H nanostructures Lead hydroxide ($Pb(OH)_2$) observed Encapsulation of lead within C-S-H	Lead leaching rate: 0.5 ppm (well below permissible limits)
		7 days	26.28	−7.27		
		14 days	27.56	−19.25		
		28 days	30.01	−20.71		
		90 days	37.85	−11.28		
		365 days	40.8	−7.96		
		730 days	41.4	−9.61		
Case 3	0.002 M lead heavy metal	3 days	23.63	−2.44	Increased Pb-C-S-H and $Pb(OH)_2$ formation Further reduction in CH peaks Visible lead deposits on C-S-H and aggregate surfaces	Lead leaching rate: 2.3 ppm (below permissible limits)
		7 days	26.38	−6.92		
		14 days	27.65	−18.99		
		28 days	31.87	−15.80		
		90 days	34.13	−20.00		
		365 days	35.21	−20.57		
		730 days	36.2	−20.96		
Case 4	0.005 M lead heavy metal	3 days	22.85	−5.66	Pronounced Pb-C-S-H and $Pb(OH)_2$ presence Minimal CH observed Lead deposits on C-S-H and aggregate surfaces	Lead leaching rate: 5.6 ppm (below permissible limits)
		7 days	25.01	−11.75		
		14 days	27.26	−20.13		
		28 days	29.62	−21.74		
		90 days	33.24	−22.08		
		365 days	34.32	−22.58		
		730 days	35	−23.58		
Case 5	0.01 M lead heavy metal	3 days	20.79	−14.16	Significant Pb-C-S-H and $Pb(OH)_2$ formation Negligible CH observed Extensive lead deposits affecting hydration products	Lead leaching rate: 14.3 ppm (below permissible limits)
		7 days	23.73	−16.27		
		14 days	25.89	−24.14		
		28 days	27.46	−27.45		
		90 days	29.32	−31.27		
		365 days	31.19	−29.64		
		730 days	31.7	−30.79		
Case 6	0.02 M lead heavy metal	3 days	19.71	−18.62	Predominant Pb-C-S-H and $Pb(OH)_2$ phases Absence of CH Lead compounds covering most cementitious phases	Lead leaching rate: 30.01 ppm (below permissible limits)
		7 days	22.36	−21.10		
		14 days	24.81	−27.31		
		28 days	26.97	−28.75		
		90 days	28.05	−34.25		
		365 days	28.13	−36.54		
		730 days	28	−38.86		
Case 7	0.05 M lead heavy metal	3 days	17.26	−28.74	Dominance of Pb-C-S-H and $Pb(OH)_2$ phases Absence of CH Porosity increase leading to severe strength loss	
		7 days	20.69	−26.99		
		14 days	22.46	−34.19		
		28 days	22.95	−39.37		
		90 days	22.54	−47.16		
		365 days	17.03	−61.58		
		730 days	14	−69.43		

Table 5. Impact of lead contamination on compressive strength and microstructural properties of concrete samples.

- Unlike earlier assumptions, the formation of ettringite structures was influenced at higher lead concentrations, showing reduced presence due to Pb-induced modifications in sulfate availability.
- XRD, SEM, and EDX analyses showed a decline in the Ca/Si and Ca/(Al + Si) ratios and an increase in the Pb/Si and Pb/(Al + Si) ratios at higher lead concentrations. This indicates the continuous incorporation of lead into the cement matrix, forming Pb-C-S-H and $Pb(OH)_2$ compounds, which led to increased porosity and reduced structural integrity over extended curing periods.
- Compressive strength increased over time in the control sample due to continued cement hydration, reaching 45.8 MPa at 730 days, confirming the long-term development of strength in uncontaminated concrete.
- However, increasing lead concentration in mixing water resulted in a significant reduction in compressive strength. For instance, at 0.05 M lead concentration, compressive strength dropped from 28.3 to 20.6 MPa at 7 days and from 42.6 to 23.5 MPa at 90 days, ultimately declining to 14 MPa at 730 days, representing a 69.4% reduction.
- In high Pb concentrations (≥ 0.01 M), long-term compressive strength exhibited severe deterioration, with reductions exceeding 30% compared to the control sample.
- Pb incorporation led to increased amorphization of C-S-H phases, reducing Ca/Si ratios and accelerating structural instability, particularly in extended curing periods.
- The highest Pb concentration (0.05 M) resulted in almost 70% strength loss after two years, highlighting significant durability concerns and limiting its practical application in structural materials.

These findings highlight the critical role of heavy metal contaminants in altering the microstructure and mechanical performance of cementitious materials, particularly in long-term exposure scenarios. This study underscores the necessity for careful assessment and mitigation strategies when utilizing lead-contaminated water in construction applications, especially for long-term durability considerations.

Data availability

All data generated or analysed during this study are included in this published article.

Received: 8 April 2025; Accepted: 12 June 2025
Published online: 02 July 2025

References

1. Ghazi, A. B., Jamshidi-Zanjani, A. & Nejati, H. Utilization of copper mine tailings as a partial substitute for cement in concrete construction. *Constr. Build. Mater.* **317**, 125921 (2022).
2. Saedi, A., Jamshidi-Zanjani, A., Mohseni, M., Darban, A. K. & Nejati, H. Mechanical activation of lead–zinc mine tailings as a substitution for cement in concrete construction. *Constr. Build. Mater.* **364**, 129973 (2023).
3. Adnan, M. et al. Heavy metals pollution from smelting activities: A threat to soil and groundwater. *Ecotoxicol. Environ. Saf.* **274**, 116189 (2024).
4. Fu, G. et al. Research on the application of lead chrome green in colored cement concrete. In *Advances in Frontier Research on Engineering Structures,* 179–191 (2024).
5. Silvestro, L. et al. Rotational rheometry test of Portland cement-based materials—A systematic literature review. *Constr. Build. Mater.* **432**, 136667 (2024).
6. Adufu, Y. D. et al. Durability behaviors of calcined kaolin clay-based geopolymer concrete containing different calcium compounds and cured in ambient sub-Saharan climate. *Constr. Build. Mater.* **465**, 140195 (2025).
7. Mehta, P. K. & Monteiro, P. *Concrete: Microstructure, Properties, and Materials* (2006).
8. Tanguler-Bayramtan, M. & Yaman, I. O. Cement and innovative sustainable binders. In *Sustainable Concrete Materials and Structures,* 9–40 (2024).
9. Tao, Y., Mohan, M. K., Rahul, A. V., De Schutter, G. & Van Tittelboom, K. Hydration and microstructure of calcium sulfoaluminate-Portland cement binder systems for set-on-demand applications. *Mater. Struct.* **57**, 35 (2024).
10. Gong, P. et al. Hydration and carbonation reaction dynamics in CO_2-rich environment for tricalcium silicate (C_3S) and dicalcium silicate (C_2S). *Powder Technol.* **452**, 120535 (2025).
11. Liu, J., Wu, D., Tan, X., Yu, P. & Xu, L. Review of the interactions between conventional cementitious materials and heavy metal ions in stabilization/solidification processing. *Materials* **16**, 3444 (2023).
12. Li, K. et al. Innovation and prospects of heavy metal solidification/stabilization techniques: A comprehensive review on materials, mechanisms, and evaluation systems. *Environ. Technol. Innov.* **37**, 104040 (2025).
13. Cartledge, F. K. et al. Immobilization mechanisms in solidifiction/stabilization of cadmium and lead salts using portland cement fixing agents. *Environ. Sci. Technol.* **24**, 867–873 (1990).
14. Taylor, H. F. *Cement Chemistry* Vol. 2 (Thomas Telford London, 1997).
15. Nawaz, K., Yu, G., Noman, M., Jintao, F. & Ahmad, W. Heavy metals stabilization in lead zinc mine tailings by using mechanical, mechano-chemical, and microwave oven activation; tailing waste utilization in building materials. *Mater. Struct.* **58**, 52. https://doi.org/10.1617/s11527-024-02567-9 (2025).
16. Chen, J. et al. Resource utilization of ultrasonic carbonated MSWI fly ash as cement aggregates: Compressive strength, heavy metal immobilization, and environmental-economic analysis. *Chem. Eng. J.* **472**, 144860 (2023).
17. Živica, V. Hardening and properties of cement-based materials incorporating heavy metal oxides. *Bull. Mater. Sci.* **20**, 677–683 (1997).
18. Komarneni, S., Breval, E., Roy, D. M. & Roy, R. Reactions of some calcium silicates with metal cations. *Cem. Concr. Res.* **18**, 204–220 (1988).
19. Wang, D. & Wang, Q. Clarifying and quantifying the immobilization capacity of cement pastes on heavy metals. *Cem. Concr. Res.* **161**, 106945 (2022).
20. Pang, F., Wei, C., Zhang, Z., Wang, W. & Wang, Z. The migration and immobilization for heavy metal chromium ions in the hydration products of calcium sulfoaluminate cement and their leaching behavior. *J. Clean. Prod.* **365**, 132778 (2022).
21. Lee, D. Formation of leadhillite and calcium lead silicate hydrate (C–Pb–S–H) in the solidification/stabilization of lead contaminants. *Chemosphere* **66**, 1727–1733 (2007).
22. Wang, B. et al. Solidification performance and mechanism of CSH gel for Pb(II), Zn(II), and Cd(II). *J. Build. Eng.* **99**, 111464 (2025).

23. Zhang, X., Wang, B. & Chang, J. Adsorption behavior and solidification mechanism of Pb(II) on synthetic CSH gel with low and high Ca/Si ratios in highly alkaline environments. *J. Environ. Chem. Eng.* **12**, 113871 (2024).
24. ASTM. *Annual Book of ASTM Standards* (American Society for Testing & Materials, 2014).
25. DIN1048. *Testing Concrete: Testing of Hardened Concrete (Specimens prepared in mould), Beton und Stahlbeton 1, Deutscher Ausschuß für Stahlbeton of the Normenausschuß Bauwesen, UDC* (1991).
26. Huff, W. D. X-ray diffraction and the identification and analysis of clay minerals, by DM Moore and RC Reynolds Jr., Oxford University Press, New York. *Clays Clay Miner.* **38**, 448–448 (1990).
27. Ouhadi, V. R. & Yong, R. Impact of clay microstructure and mass absorption coefficient on the quantitative mineral identification by XRD analysis. *Appl. Clay Sci.* **23**, 141–148 (2003).
28. Yoo, H. & Lee, D. The microstructure of Pb-doped solidified waste forms using Portland cement and calcite. *Environ. Eng. Res.* **11**, 54–61 (2006).
29. Zhu, K., Wang, L., Liao, L., Bai, Y. & Hu, J. Study on synthesis of CSH gel and its immobilization of heavy metals. *Crystals* **14**, 864 (2024).
30. Wang, Z. et al. Role of polyferric sulphate in hydration regulation of phosphogypsum-based excess-sulphate slag cement: A multiscale investigation. *Sci. Total Environ.* **948**, 173750 (2024).
31. Ouki, S. & Hills, C. Microstructure of Portland cement pastes containing metal nitrate salts. *Waste Manag.* **22**, 147–151 (2002).
32. Amiri, M., Sanjari, M. & Porhonar, F. Microstructural evaluation of the cement stabilization of hematite-rich red soil. *Case Stud. Constr. Mater.* **16**, e00935 (2022).
33. Devamani, R. & Alagar, M. Synthesis and characterization of lead(II) hydroxide nanoparticles. *Int. J. Appl. Sci. Eng. Res.* **1**, 483–487 (2012).
34. Xu, L. et al. Lead retardation on cement hydration: Inhibition and re-acceleration of clinker dissolution. *Cement Concr. Compos.* **138**, 104986 (2023).
35. Xu, B., Winnefeld, F., Ma, B., Rentsch, D. & Lothenbach, B. Influence of aluminum sulfate on properties and hydration of magnesium potassium phosphate cements. *Cem. Concr. Res.* **156**, 106788 (2022).
36. Chen, L., Nakamura, K. & Hama, T. Review on stabilization/solidification methods and mechanism of heavy metals based on OPC-based binders. *J. Environ. Manag.* **332**, 117362 (2023).
37. Deschner, F. et al. Hydration of Portland cement with high replacement by siliceous fly ash. *Cem. Concr. Res.* **42**, 1389–1400 (2012).
38. Olmo, I. F., Chacon, E. & Irabien, A. Influence of lead, zinc, iron(III) and chromium(III) oxides on the setting time and strength development of Portland cement. *Cem. Concr. Res.* **31**, 1213–1219 (2001).

Acknowledgements
The authors would like to thank the Kharazmi University, which supported the expenses for all the tests conducted in this study.

Author contributions
S.G. Conceptualization, investigation, methodology, validation, formal analysis, writing. P.H. Review and editing; supervision, investigation, resources, formal analysis, methodology. J.K.G. Visualization, review and editing.

Funding
This research was funded by the Kharazmi University of Iran (2024Kh487654).

Declarations

Competing interests
The authors declare no competing interests.

Ethical Approval
As the corresponding author on behalf of all the authors, we assure you that this manuscript has not been submitted to another journal simultaneously.

Consent to participate
All authors agree to publish the article.

Consent to publish
All authors agree to publish the article.

Additional information
Correspondence and requests for materials should be addressed to S.G. or P.H.